Journal of Colloid and Interface Science **245,** 371–382 (2002)
doi:10.1006/jcis.2001.8031, available online at http://www.idealibrary.com on IDEAL®

Kinetics of Solubilization of *n*-Decane and Benzene by Micellar Solutions of Sodium Dodecyl Sulfate

P. D. Todorov,* P. A. Kralchevsky,*,[1] N. D. Denkov,* G. Broze,† and A. Mehreteab‡

*Laboratory of Chemical Physics & Engineering, Faculty of Chemistry, University of Sofia, 1164 Sofia, Bulgaria; †Colgate-Palmolive R&D, Inc., Avenue du Parc Industriel, B-4041 Milmort (Herstal), Belgium; and ‡Colgate-Palmolive Technology Center, Piscataway, New Jersey 08854-5596

Received June 12, 2001; accepted October 5, 2001

We observed the diminishing of single microscopic oil drops to study the kinetics of solubilization of *n*-decane and benzene by micellar solutions of sodium dodecyl sulfate (SDS). Each drop is located in a horizontal glass capillary of inner diameter 0.06 cm filled with a thermostated surfactant solution; the small vertical dimension of the cell prevents the appearance of uncontrollable thermal convections. The experiments show that the radius of an *n*-decane drop decreases linearly with time, whereas for benzene this dependence is nonlinear. To interpret the data, a kinetic model of solubilization is developed. It accounts for the diffusion and capturing of dissolved oil molecules by the surfactant micelles, as well as for the finite rate of oil dissolution at the oil-water interface. By processing the data, we determined the rate constant of solubilization for a given oil and surfactant. It turns out that the elementary act of catching a dissolved oil molecule by a surfactant micelle occurs under a barrier (rather than diffusion) control. The effective rate of solubilization is greater for the oil, which exhibits a higher equilibrium solubility in pure water (benzene), despite the lower value of the solubilization rate constant for this oil.

Key Words: **benzene; *n*-decane; sodium dodecyl sulfate; solubilization kinetics; solubility of oil in water; surfactant micelles.**

1. INTRODUCTION

Two major mechanisms of solubilization of oil by surfactant micelles are distinguished in the literature: (A) *Surface reaction*: the solubilization is effectuated through a transient adsorption of surfactant micelles at the water-oil interface (1–7). (B) *Bulk reaction*: the surfactant micelles can capture oil molecules dissolved in the aqueous phase (3, 4, 8, 9–11). Mechanism (A) could be operative with oils, like triglycerides, which are practically insoluble in water. In contrast, mechanism (B) can be observed only with oils which do exhibit some solubility in water. In the intermediate case of hydrocarbons, which have a sufficiently low solubility in water, both mechanisms could be simultaneously operative.

It is important to note that the occurrence of mechanism (A) can be completely suppressed if there is an electrostatic (double layer) repulsion between micelles and oil drops. This is the situation when ionic surfactants are present in the solution. For example, in some of our experiments (12) we observed that micellar solutions of the nonionic surfactant $C_{12}EO_6$ (polyoxyethylene-6 lauryl ether) are able to solubilize triolein in the presence of 0.2 M Na_2SO_4 at 27°C. However, it was sufficient to add only a small fraction (20 molar % in the surfactant mixture) of the ionic surfactant sodium dodecyl dioxyethylene sulfate, SDP2S, to cause a complete ceasing of the solubilization. Note that even the giant rodlike micelles of SDP2S, obtained in the presence of $AlCl_3$, are not able to solubilize triglycerides, although these micelles readily solubilize oils like xylene and di(isopropyl) benzene (13).

In the present article we investigate the kinetics of solubilization of *n*-decane and benzene by micellar solutions of SDS (sodium dodecyl sulfate). These hydrocarbons exhibit a finite molecular solubility in water; the respective equilibrium concentrations are $c_{eq} = 1.11 \times 10^{-6}$ and 2.28×10^{-2} M at 25°C (14). Since SDS brings a considerable surface charge to both micelles and oil drops, we expect that they repel each other; consequently, the occurrence of mechanism (A) is completely suppressed. Therefore, we assume that in our experiments the solubilization follows mechanism (B). The goal of our kinetic measurements is to determine the rate constant, k_+, of the reaction {micelle} + {oil molecule} = {swollen micelle}, as well as to find the mass transfer coefficient, α, for the oil molecules across the oil-water interface. These two parameters can be determined by processing the experimental data with the help of an adequate theoretical model. So, our first task was to design an experimental procedure, which provides data liable to a trustworthy theoretical interpretation.

When the solubilization experiment is carried out with batch emulsions, complex collective phenomena are observed (15–17). The simultaneous occurrence of two opposing physical processes has been observed: decrease of the drop size and number concentration, due to micellar solubilization, and an increase of the mean drop size due to Ostwald ripening (15–17). To simplify the experimental system, following Miller *et al.* (6, 18, 19) we made experiments with individual oil drops in an immobile aqueous surfactant solution. In such case, the transport of oil molecules and micelles is effectuated only by diffusion, which can be easily modeled theoretically. However, one

[1] To whom correspondence should be addressed. E-mail: pk@lcpe.uni-sofia.bg.

0021-9797/02 $35.00

should take special measures to avoid uncontrollable thermal convections, which could completely prevail (if present) over the slow diffusion in the mass transport. Even a slow thermal convection may cause a misinterpretation of kinetic experimental data (20). A criterion about the presence or absence of such convection is provided by the Rayleigh number, $R_h \equiv g\beta\Theta h^3/(\nu\chi)$:

$$R_h \leq 1 \rightarrow \text{ no thermal convection}$$
$$R_h > 1 \rightarrow \text{ there is thermal convection;}$$

see, e.g., Ref. (21); here h is the height of the liquid in the vessel, g is the acceleration due to gravity, $\beta = 2.27 \times 10^{-4}$ K^{-1} is the coefficient of thermal expansion of water, Θ is the characteristic temperature difference, $\nu \approx 8.2 \times 10^{-3}$ cm^2/s is kinematic viscosity of water, $\chi \approx 1.44 \times 10^{-3}$ cm^2/s is the temperature conductivity of water. It is worthwhile noting that even with a very fine control of the temperature, $\Theta \approx 0.02^\circ$ K, the Rayleigh number is rather large for a vessel of height $h = 5$ cm, $R_h = 4.7 \times 10^4$, and considerable thermal convections take place. Hence, it is virtually impossible to suppress the thermal convections by thermostating large vessels. Instead, one could successfully suppress the free convections by decreasing the vertical dimension of the vessel, h (20).

The article is structured as follows. In the next section we describe the experimental setup, procedure, and results. Further, we develop a theoretical model and consider the limiting cases of narrow and wide solubilization zone, corresponding to *n*-decane and benzene, respectively. Next, we compare the theory with experiment, and determine the solubilization rate constant and the mass transfer coefficient for the boundary oil-water. Finally, we discuss the relationship between the molecular solubility of oil in water and the rate constant of solubilization.

2. EXPERIMENT

2.1. Experimental Setup and Procedure

The experimental technique for studying the kinetics of solubilization of single oil drops was first used in Ref. (12) to examine the solubilization of triglycerides in micellar solutions of nonionic surfactants. The surfactant solution is loaded in a glass capillary of inner diameter 600 μm. For this purpose, one of its ends is immersed in the surfactant solution, which spontaneously fills the tube due to the capillary-rise effect. The capillary is inserted in a special cylindrical channel drilled in the thermostated metal block of the experimental setup (Fig. 1). An oil drop is injected in the capillary by means of a microsyringe with a fine glass needle of outer diameter 45 μm. Next, the two ends of the capillary are plugged to prevent evaporation of the solution. During the experiment, the capillary is held in the horizontal cylindrical channel; the temperature is maintained at 27°C. The metal block has four parallel channels, which allow simultaneous experiments with four capillaries. Above each capillary, there is an opening, covered with an optical glass plate, which enables one

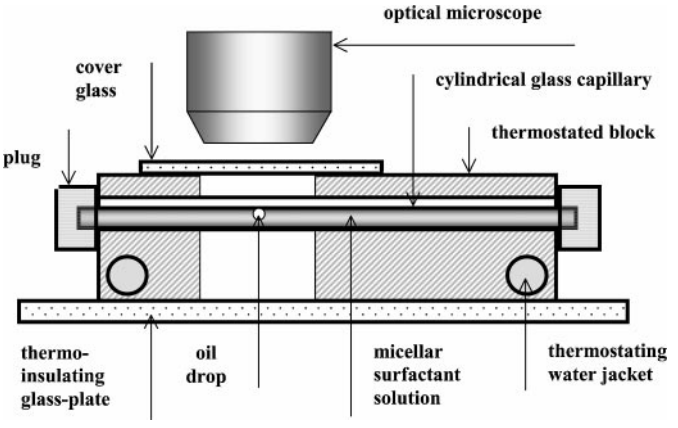

FIG. 1. The experimental setup for studying the kinetics of solubilization of a single oil drop. The diameter of the diminishing drop is recorded as a function of time.

to observe the oil drops by optical microscope (Fig. 1). Thus, the diminishing of each oil drop, due to solubilization, can be recorded as a function of time. The capillaries are precleaned by consecutively filling them with several portions of chromic acid, followed by abundant rinsing with deionized water.

The relatively small inner diameter of the capillary and its horizontal position prevent the appearance of free thermal convections in the surfactant solution; the calculated Rayleigh number is $R_h = 0.8$. Thus, the solubilization occurs in a regime of diffusion mass transfer. If some uncontrollable thermal convections were present, they would make it impossible to quantitatively interpret the experimental data (20).

As already noted, in our experiments we used aqueous solutions of SDS (product of Fluka); the oils were pure benzene and *n*-decane (Sigma). It is known that the spherical SDS micelles have an average aggregation number $n_m = 67$ and radius $r_m = 2.4$ nm (22). In the absence of added salt, the transition from spherical to elongated (cylindrical) micelles occurs at SDS concentration 0.25 M at temperature 27°C (22). In our experiments we worked with SDS concentrations $\leq$0.25 M.

2.2. Experimental Results

Figure 2 shows illustrative experimental data for the diminishing of 5 *n*-decane drops owing to the solubilization in SDS micellar solutions. One sees that the drop radius R decays *linearly* with the time t, in the investigated range of sizes. In addition, the slope of the experimental lines (that is, the rate of solubilization) systematically increases with the rise of the SDS concentration. On the other hand, Fig. 3 demonstrates that the slope of the lines $R(t)$ is practically independent of the initial drop size for a fixed SDS concentration.

For SDS concentrations below the CMC, the drops of *n*-decane did not show any change of size within 1 week. In other words, the rate of molecular dissolution of *n*-decane in water is completely negligible in comparison with the rate of micellar solubilization.

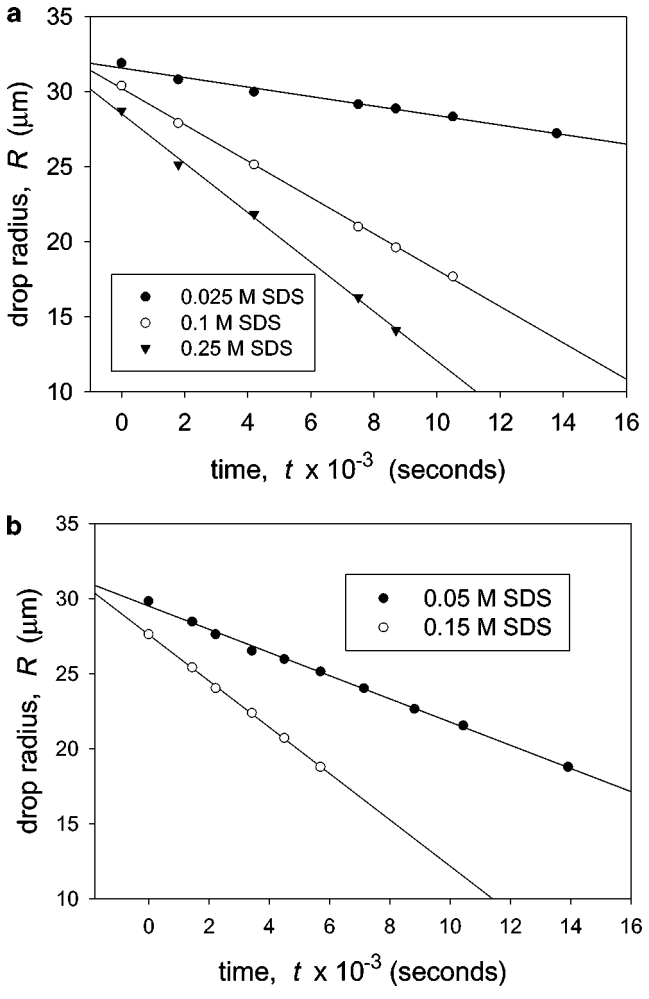

FIG. 2. Plot of the radius, R, vs time, t, for n-decane drops in micellar SDS solutions at 27°C (SDS concentrations denoted in the figure). Each line corresponds to a separate diminishing drop; the linear regressions are drawn in accordance with Eq. [17] and the respective values of u are listed in Table 2.

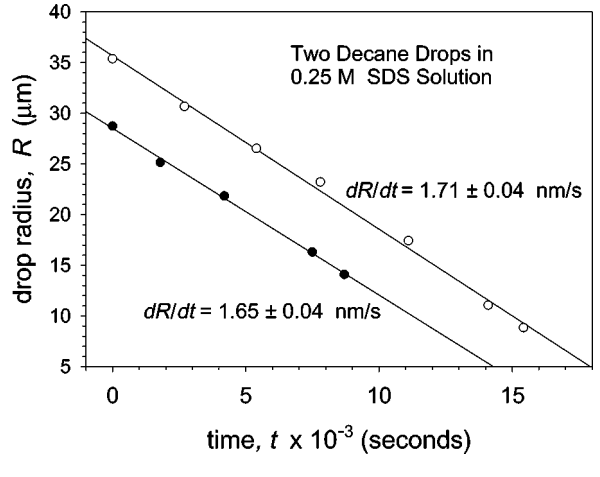

FIG. 3. Plot of the radius, R, vs time, t, for two drops of n-decane in 0.25 M solution of SDS at 27°C.

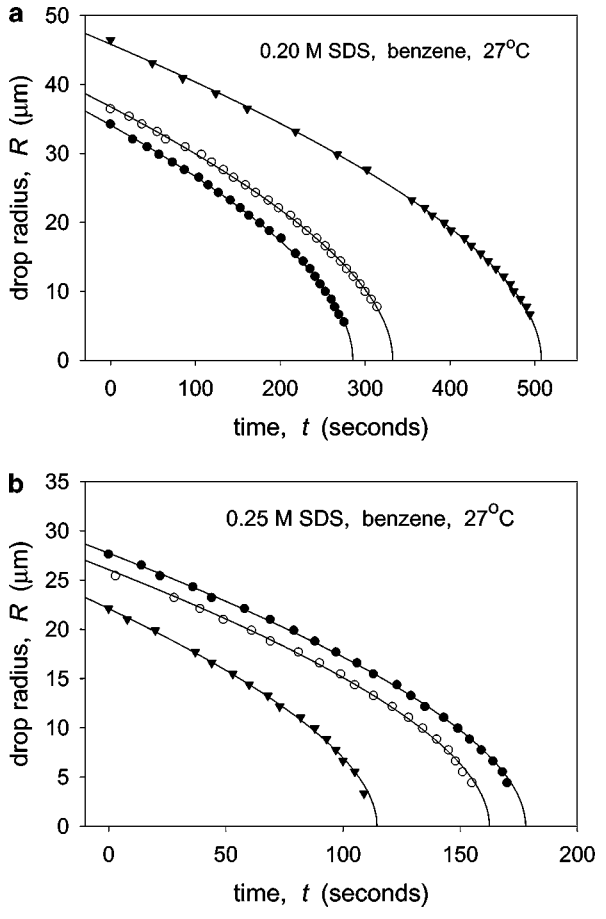

FIG. 4. Plot of the radius, R, vs time, t, for benzene drops in micellar SDS solutions at 27°C; (a) 0.20 M SDS; (b) 0.25 M SDS. Each curve corresponds to a separate diminishing drop; the theoretical fits are drawn with the help of Eq. [24] (see also Tables 3 and 4).

Figure 4 presents typical experimental $R(t)$ dependencies for 6 benzene drops of various initial size at two surfactant concentrations: 0.20 and 0.25 M SDS. In contrast with the experimental curves for n-decane (Figs. 2 and 3), the plots $R(t)$ are *nonlinear* for benzene. Moreover, the rate of drop diminishing is $|dR/dt|$ >70 nm/s for benzene, whereas it is much lower for n-decane, $|dR/dt|$ <3 nm/s. Examining more closely the curves in Fig. 4 one may conclude that the slope $|dR/dt|$ is greater for the higher micelle concentration at a given R.

Figure 5 shows data for the diminishing of a benzene drop in a 0.007 M SDS solution, i.e., below the CMC (no micellar solubilization). This experimental curve demonstrates that the rate of molecular dissolution of benzene in water is significant. The comparison between the $R(t)$ curves corresponding to 0.007 and 0.25 M SDS shows that the micellar solubilization accelerates the diminishing of the benzene drops, as expected. The rate of micellar solubilization becomes comparable with the rate of molecular dissolution only for the highest studied SDS concentrations, around 0.25 M; for lower SDS concentrations the molecular dissolution prevails.

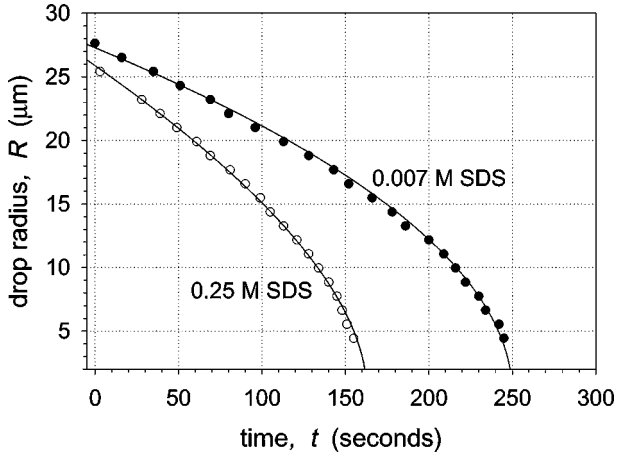

FIG. 5. Plot of the radius, R, vs time, t, for two benzene drops in SDS solutions at 27°C; 0.007 M SDS is just below the CMC and the fit is drawn by means of Eq. [23]; 0.25 M SDS is about 30 times CMC and the fit is drawn by means of Eq. [24].

To interpret the obtained experimental data (Figs. 2–5), in the next section we propose a theoretical model.

3. THEORETICAL MODEL

3.1. Basic Equations

Let us assume that up to M oil molecules can be incorporated in a micelle. The total micelle concentration is

$$c_{\rm tot} = \sum_{n=0}^{M} c_n, \qquad [1]$$

where c_n is the concentration of micelles which contain n incorporated oil molecules. Let us consider the solubilization as an irreversible reaction:

$$\mathrm{A}_n + \mathrm{O} \rightarrow \mathrm{A}_{n+1}, \quad n = 0, 1, \ldots, M-1. \qquad [2]$$

Here O and A_n symbolize, respectively, an oil molecule and a micelle containing n incorporated oil molecules. The treatment of solubilization as an *irreversible* reaction, at least in its initial stages (predominantly empty micelles in the bulk), is supported by the achieved good agreement between the respective theoretical predictions and the experimental results: see Fig. 2 in Ref. (9) and Fig. 6 in Ref. (23). The concentration of *active* micelles, i.e., micelles which are able to solubilize oil, is

$$c_a = \sum_{n=0}^{M-1} c_n = c_{\rm tot} - c_M. \qquad [3]$$

c_M is the concentration of the *full* micelles, which cannot incorporate additional oil molecules. If the solubilization occurs in a stationary regime, the concentration of dissolved oil, $c_{\rm oil}$, obeys the equation

$$D_{\rm oil}\nabla^2 c_{\rm oil} = k_+ c_a c_{\rm oil}, \qquad [4]$$

where $D_{\rm oil}$ is the diffusivity of oil molecules dissolved in water, and k_+ is the rate constant of solubilization. Following Kabalnov and Weers (9), we have used in Eq. [4] the approximation that the rate constant k_+ is the same for all active micelles. Further, for spherical symmetry, Eq. [4] can be represented in the form

$$\frac{1}{r^2}\frac{d}{dr}\left(r^2\frac{dc_{\rm oil}}{dr}\right) = \kappa^2 c_{\rm oil}, \qquad [5]$$

$$\kappa^2 = k_+ c_a / D_{\rm oil}. \qquad [6]$$

If the micelle diffusion is sufficiently fast (in comparison with the process of solubilization), then one can expect that the active micelles leave the neighborhood of the oil drop before becoming full micelles. In such case, the concentration of the full micelles is zero, $c_M(r) \equiv 0$. Consequently, $c_a = c_{\rm tot} = $ const., and then Eq. [6] acquires the form

$$\kappa^2 = k_+ c_{\rm tot} / D_{\rm oil} = \text{const.} \qquad [7]$$

The boundary conditions for Eq. [5] are

$$-\left.\frac{\partial c_{\rm oil}}{\partial r}\right|_{r=R} = \alpha[c_{\rm eq} - c_{\rm oil}(R)], \quad c_{\rm oil}|_{r\rightarrow\infty} = 0, \qquad [8]$$

where $c_{\rm eq}$ is the equilibrium solubility of the oil in water and α is a mass-transfer coefficient. (Equation [8], and the subsequent theoretical expressions, are different from those in Ref. (9), where a boundary condition for a stagnant layer is imposed.) If Eq. [7] holds, then the solution of Eq. [5], along with the boundary conditions [8], reads

$$c_{\rm oil}(r) = \frac{c_{\rm eq} R}{1 + (\kappa + R^{-1})/\alpha}\frac{\exp[\kappa(R-r)]}{r}. \qquad [9]$$

Equation [9] shows that the quantity κ^{-1} determines the width of the "active zone" around the drop surface, where the solubilization takes place (see Fig. 6).

The assumption for stationary regime is valid if the diminishing of the oil drop is much slower than the solubilization process in the active zone, that is, if the following criterion is satisfied

$$K \equiv \frac{\tau_\kappa}{\tau_R} = \frac{|dR/dt|_{t=0}}{R_0\kappa^2 D_{\rm oil}} \ll 1 \quad (R_0 \equiv R(0)). \qquad [10]$$

Here, $\tau_R = R_0/|dR/dt|_{t=0}$ is the characteristic time of diminishing of the oil drop; $\tau_\kappa = (\kappa^2 D_{\rm oil})^{-1}$ is the characteristic time of oil diffusion across the zone of solubilization. Taking typical values for the investigated solutions, we calculate $K \approx 7\times10^{-10}$ for n-decane, and $K \approx 9\times10^{-3}$ for benzene. Hence,

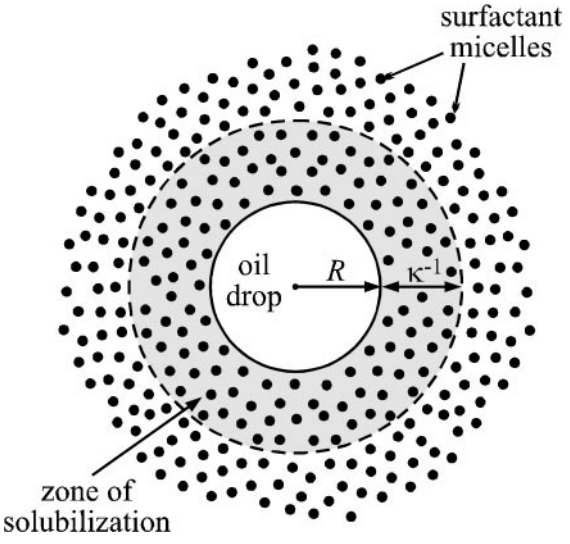

FIG. 6. Sketch of an oil drop of radius R in a micellar surfactant solution. The solubilization takes place mostly in a zone of width κ^{-1} around the drop.

the assumption for stationary regime is satisfied not only for *n*-decane, but also for benzene. (It is possible the criterion [10] to be violated for very small drops, $R_0 \to 0$; however, in our experiments we worked with sufficiently large drops, $R \geq 5\ \mu$m.)

With the help of Eq. [9] one determines that the number of oil molecules dissolved in water per unit area of the drop surface, and per unit time, is

$$Q_{\rm oil} = -D_{\rm oil}\frac{\partial c_{\rm oil}}{\partial r}\bigg|_{r=R} = \frac{\kappa + R^{-1}}{1 + (\kappa + R^{-1})/\alpha} D_{\rm oil} c_{\rm eq}. \quad [11]$$

The decrease of the volume of the oil drop, V, with the time, t, can be expressed in the form

$$-\frac{dV}{dt} = {\rm v}_{\rm oil}(4\pi R^2)\lambda Q_{\rm oil}. \quad [12]$$

Here $\rm v_{oil}$ is the volume per molecule in the oil phase and λ is a geometrical correction factor, which accounts for the fact that in our experiments the oil drop is located below the glass surface (the surface of the capillary, see Fig. 1), rather than in the bulk of the aqueous phase. In the appendix we show that λ depends on the product κR, see Eq. [A13]. For our needs λ can be approximated with the expression

$$\lambda = \frac{0.9 + 4.725\kappa R + 2.1(\kappa R)^2}{1 + 5.25\kappa R + 2.1(\kappa R)^2}. \quad [13]$$

Note that $0.9 \leq \lambda \leq 1$ (details are given in the appendix). Substituting Eq. [11] and $V = \frac{4}{3}\pi R^3$ in Eq. [12], we obtain a differential equation for $R(t)$,

$$\frac{dR}{dt} = -\frac{\alpha\beta(1+\kappa R)}{1 + (\alpha + \kappa)R}\lambda(\kappa R), \quad [14]$$

where β is a parameter which is determined by the properties of the oil:

$$\beta = {\rm v}_{\rm oil} D_{\rm oil} c_{\rm eq}. \quad [15]$$

By integration of Eq. [14] one can obtain the theoretical dependence $R(t)$.

3.2. Limiting Case $\kappa R \gg 1$

In the limit $\kappa R \gg 1$, corresponding to a narrow zone of solubilization around the oil drop (see Fig. 6), $\lambda = 1$ and Eq. [14] reduces to

$$-\frac{dR}{dt} \approx \frac{\alpha\beta\kappa}{\alpha + \kappa} \equiv u \quad (\kappa R \gg 1), \quad [16]$$

where the constant parameter u has the meaning of solubilization rate. Integrating Eq. [16] with a boundary condition $R(0) = R_0$, we get

$$R(t) \approx R_0 - ut \quad (\kappa R \gg 1) \quad [17]$$

Equation [17] can be used to interpret the linear dependencies $R(t)$ obtained in our experiments with drops of *n*-decane, see Figs. 2 and 3. The slopes of the experimental lines give u as a function of the surfactant concentration, c_s. In view of Eqs. [7] and [16] one obtains

$$u = \frac{ax}{b + x}, \quad x = (c_s - c_{s0})^{1/2}, \quad [18]$$

where

$$a = \alpha\beta, \quad b = (D_{\rm oil} n_{\rm m} \alpha^2 / k_+)^{1/2}. \quad [19]$$

$n_{\rm m}$ is the mean aggregation number of the micelles; as noted above, for SDS without added salt $n_{\rm m} \approx 67$. The total number concentration of the active micelles is

$$c_{\rm tot} = (c_s - c_{s0})/n_{\rm m}, \quad [20]$$

where c_s is the total surfactant concentration in the solution and c_{s0} is the value of c_s, at which active micelles (able to solubilize the respective oil) appear in the solution.

3.3. Limiting Case $\alpha\kappa^{-1} \gg 1$

Since r scales with κ^{-1}, Eq. [8] can be represented in the form

$$\frac{1}{\alpha\kappa^{-1}}\frac{\partial c_{\rm oil}}{\partial \tilde{r}}\bigg|_{r=R} = c_{\rm oil}|_{r=R} - c_{\rm eq}, \quad (\tilde{r} = \kappa r). \quad [8a]$$

In the limit $\alpha\kappa^{-1} \gg 1$ the left-hand side of Eq. [8a] vanishes and one obtains

$$c_{\text{oil}}|_{r=R} = c_{\text{eq}}, \quad (\alpha\kappa^{-1} \gg 1) \tag{21}$$

Equation [21] means that for $\alpha\kappa^{-1} \gg 1$ the subsurface concentration (that in a close vicinity of the oil-drop surface) is constant and equal to the equilibrium concentration of dissolved oil in water. Such situation could be expected for oils, like benzene, which exhibit a pronounced solubility in water. Further, in the same limit, $\alpha \to \infty$, Eq. [14] reduces to

$$\frac{dR}{dt} = -\frac{\beta}{R}(1 + \kappa R)\lambda(\kappa R). \tag{22}$$

In the case of narrow solubilization zone, $\kappa R \gg 1$ (see Fig. 6), Eq. [22] yields $dR/dt \propto \kappa$, that is, the rate of oil dissolution is dominated by the micellar solubilization. In the opposite case of wide solubilization zone, $\kappa R \ll 1$, Eq. [22] gives $dR/dt \propto R^{-1}$, and then the rate of diminishing of the oil drop is determined by the molecular dissolution of oil in water.

Let us first consider the simpler case of purely molecular dissolution of oil in water (no micellar solubilization). Setting $\kappa = 0$ in Eq. [22] and integrating, one obtains ($\lambda = 0.9$, see Eq. [13])

$$R(t) = \sqrt{1.8\beta(t_0 - t)} \quad (\kappa \ll R^{-1}), \tag{23}$$

where t_0 denotes the moment of disappearance of the drop, $R(t_0) = 0$.

In the more general case of simultaneous molecular dissolution and micellar solubilization, we integrate Eq. [22] using Eq. [13] for λ; it is convenient to present the result in the form

$$t(R) = t_0 - \frac{1}{\beta\kappa^2}G(\kappa R), \tag{24}$$

where

$$G(x) = \int_0^x \frac{\xi\, d\xi}{(1+\xi)\lambda(\xi)} \approx x - 1.2464\ln(1+x) + 0.4957 \times \ln\left(1 + \frac{x}{2.04}\right) + 7.16 \times 10^{-4}\ln\left(1 + \frac{x}{0.21}\right). \tag{25}$$

Since $\lambda(\xi)$ appears under the sign of an integral, the computed $G(x)$ is numerically almost the same irrespective of whether the exact expression, Eq. [A13], or the approximate one, Eq. [13], is used. Equation [24] expresses the inverse of the dependence $R(t)$, viz. $t(R)$. Note that β is a known material parameter, see Table 1. In the next section, Eq. [24] is used to fit the experimental curves for benzene drops (Figs. 4 and 5) using κ as an adjustable parameter. From the value of κ, determined from the best fit, one can calculate the rate constant of solubilization,

$$k_+ = \kappa^2 D_{\text{oil}}/c_{\text{tot}}, \tag{26}$$

cf. Eq. [7].

TABLE 1
Properties of the Oils Used in the Experiments

Parameter	*n*-Decane	Benzene
Mass density (g/cm^3)	0.73	0.87
v_{oil} (cm^3)	3.23×10^{-22}	1.49×10^{-22}
D_{oil} (cm^2/s)	7.8×10^{-6}	8.1×10^{-6}
c_{eq} (cm^{-3})	6.69×10^{14}	1.37×10^{19}
β(cm^2/s)	1.686×10^{-12}	1.654×10^{-8}

4. COMPARISON OF THEORY AND EXPERIMENT

4.1. Fits of the Experimental Data for n-Decane

The values of the equilibrium molecular solubilities, c_{eq}, of *n*-decane and benzene in water differ by several orders of magnitude, see Table 1 and Ref. (14). The experimental data for the solubilization of decane drops (see Fig. 2) are fitted by straight lines in accordance with Eq. [17]. The values of the determined slope of the lines, u, which characterizes the rate of solubilization, are listed in Table 2. Figure 7 shows the plot of u vs $(c_s - c_{s0})^{1/2}$ in accordance with Eq. [18]. From the best fit we determined the following parameter values:

$$a = 5.02 \pm 0.98\,(\text{nm/s}), \quad b = 0.87 \pm 0.24\,(\text{M}^{1/2}), \quad c_{s0} = 0.013 \pm 0.001\,(\text{M}). \tag{27}$$

The latter value of c_{s0} is somewhat larger than the CMC of SDS, 0.008 M. In fact, c_{s0} is the value of CMC determined by solubilization experiments. The result that c_{s0} is larger than the CMC obtained by surface-tension measurements is not so surprising, insofar as it is known that different experimental methods, including light scattering, electroconductivity, osmotic pressure, density change, and detergency, often give different values for the CMC, see, e.g., Fig. 2.1 in Ref. (24).

From the above values of a and b, with the help of Eq. [19], we determine the mass-transfer coefficient, α, and the rate constant

TABLE 2
Results from the Fits of the Data for *n*-Decane

c_s(M)	u(nm/s)	κ^{-1}(μm)
0.025	0.31	0.267
0.05	0.77	0.152
0.10	1.21	0.099
0.15	1.54	0.079
0.20	1.68	0.067
0.25	1.71	0.061

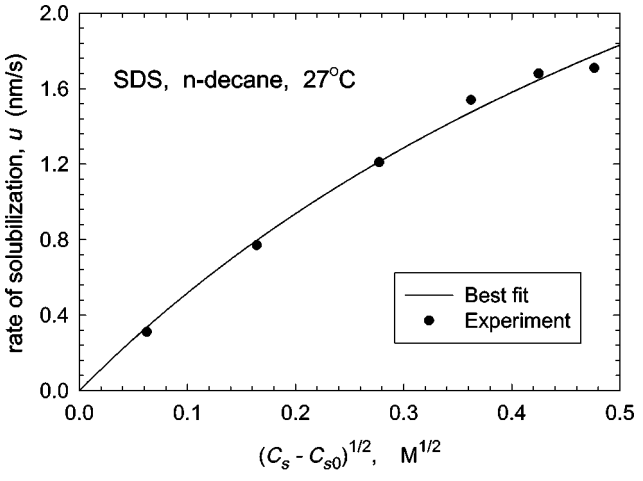

FIG. 7. The experimental rate of solubilization, $u = |dR/dt|$, plotted vs $(c_s - c_{s0})^{1/2}$ in accordance with Eq. [18].

of solubilization, k_+:

$$\alpha = a/\beta = 29.8 \pm 5.8\,(\mu\mathrm{m}^{-1}) \qquad [28]$$

$$k_+ = D_{\mathrm{oil}} n_{\mathrm{m}} \left(\frac{a}{\beta b}\right)^2 = (1.02 \pm 0.34) \times 10^{-13}\,(\mathrm{cm}^3/\mathrm{s}). \qquad [29]$$

Next, using the latter value of k_+, with the help of Eqs. [7] and [20] we calculate the width of the solubilization zone, κ^{-1}, which is also listed in Table 2. One sees, that for decane κ^{-1} is really much smaller than the drop radius R, as assumed in Section 3.2; see also Fig. 6. (In our experiments usually $R \geq 10\ \mu$m, see Figs. 2 and 3).

For the decane drops, the effect of the mass transfer coefficient, α, is significant, especially for the higher SDS concentrations, for which the product $\alpha\kappa^{-1}$ is on the order of 1. (Note that α disappears from Eq. [16] only if $\alpha\kappa^{-1} \gg 1$.) Physically $\alpha\kappa^{-1} \approx 1$ means that the rate of molecular dissolution of decane at the drop surface is comparable with the rate of oil solubilization. This brings about a lowering of the subsurface concentration of decane, $c_{\mathrm{oil}}(R)$, in comparison with the equilibrium concentration of dissolved decane in water, c_{eq}, cf. Eq. [8].

4.2. Fits of the Experimental Data for Benzene

The theoretical fit of the data for 0.007 M SDS (below the CMC) in Fig. 5 is drawn by means of Eq. [23] using a single adjustable parameter, t_0; the value of β is known—see Table 1. In fact, the variation of t_0 is equivalent to a horizontal shift of the theoretical curve along the t axis. The excellent agreement between the theoretical curve and the experimental data (Fig. 5) shows that Eq. [23] really provides an adequate description of the molecular dissolution of benzene for surfactant concentrations below the CMC.

The fits of the data in Fig. 4 are drawn by means of Eq. [24]. The least-squares method has been applied with two adjustable parameters: κ and R_0; their values, corresponding to the best fit, are listed in Tables 3 and 4. The values of k_+, listed in the tables, are calculated from the value of κ with the help of Eqs. [20] and [26] using the parameter values $n_{\mathrm{m}} = 67$, $c_{s0} = 0.008$ M, and $D_{\mathrm{oil}} = 8.1 \times 10^{-6}$ cm^2/s. If the theoretical model is adequate to the experimental situation, then the computed k_+ should be independent of the initial drop size and the surfactant concentration.

TABLE 3
Results for Solubilization of Benzene in Solution of 0.25 M SDS

Drop No.	R_0 (μm)	κ^{-1}(μm)	k_+(nm^3/s)
Drop 1	27.8	41.3	218
Drop 2	27.7	40.5	227
Drop 3	26.1	45.0	184
Drop 4	22.1	33.6	331
Average	—	40.1	232

In general, Eq. [24] provides excellent fits of the experimental curves for all examined benzene drops. However, the reproducibility of the values of κ and k_+, obtained from the fits for different drops in the same solution, worsens with the decrease of the micelle concentration. Also, k_+ is lower for 0.2 M SDS. These results could be attributed to the following two factors.

(i) The micellar solubilization of benzene drops appears on the background of an intensive molecular dissolution (see Fig. 5). Of course, both these effects are taken into account in our model. However, for not too high micelle concentrations the molecular dissolution certainly prevails over the micellar solubilization. In such case, the solubilization has only a small contribution to the observed drop diminishing, and consequently, the parameter κ is determined with a relatively large experimental error from the fits of the data for $R(t)$.

(ii) Due to the relatively high concentration of the benzene molecules in the solubilization zone, and the relatively large width of the latter (cf. the values of R_0 and κ^{-1} in Tables 2 and 3) it is possible for "full micelles" to appear. In other words, a part of the micelles will become "full" (unable to incorporate additional oil) before they leave the solubilization zone (Fig. 6) by diffusion. This will result in a decrease of the concentration of the "active micelles" and will decelerate the solubilization. However, in our model we have neglected the concentration of the full micelles, see Section 3.1; therefore, the deceleration of the solubilization will lead to lower effective values of the rate constant k_+ determined from the data fits.

Hence, the existence of "full micelles" could be the explanation of the smaller values of k_+ in Table 4 in comparison with

TABLE 4
Results for Solubilization of Benzene in Solution of 0.20 M SDS

Drop No.	R_0 (μm)	κ^{-1} (μm)	k_+ (nm^3/s)
Drop 1	34.1	61.4	125
Drop 2	36.7	66.2	107
Drop 3	45.8	77.5	78

those in Table 3. Moreover, higher concentrations of "full micelles," and smaller effective values of k_+, are expected for the drops of greater initial radius R_0, which supply a greater amount of benzene to their aqueous environment in the process of their dissolution. Such a tendency is present for the drops in 0.2 M SDS solution, see Table 4: k_+ is smaller for the drops with larger R_0.

The most reproducible data are those obtained with 0.25 M SDS solutions (Table 3). Consequently, the most reliable value of the solubilization rate constant for the system benzene/SDS is the average value in Table 3, viz. $k_+ \approx 2.3 \times 10^{-19}$ cm^3/s.

5. DISCUSSION

5.1. Diffusion or Barrier Control

First, let us consider the kinetic mechanism of the elementary act of solubilization, that is, the reaction of a surfactant micelle with an oil molecule dissolved in water, Eq. [2]. If this reaction were limited by diffusion, then k_+ would be given by the expression (9)

$$k_+ = 4\pi D_{\text{oil}}\, r_m \quad \text{(diffusion control)}, \qquad [30]$$

where $r_m \approx 2.4$ nm is the hydrodynamic radius of the SDS micelles (22). With the values for D_{oil} in Table 1, Eq. [30] predicts $k_+ \approx 2.4 \times 10^{-11}$ cm^3/s for both *n*-decane and benzene. The latter value is by orders of magnitude greater than our results for k_+ in Eq. [29] and Table 3. Hence, we may conclude that in our case the elementary act of solubilization happens under *barrier* control.

In addition, our results show that the rate constant for *n*-decane, $k_+ \approx 1.0 \times 10^{-13}$ cm^3/s, is much greater than that for benzene, $k_+ \approx 2 \times 10^{-19}$ cm^3/s. In other words, the barrier to solubilization is much higher for benzene in comparison with *n*-decane. Despite this large difference between the rate constants, benzene dissolves faster in micellar solutions than *n*-decane. The reason for this striking fact is discussed below.

5.2. Solubilization Rate Constants and Molecular Solubility of Oils

As noted above, Eq. [29] and Table 3 show that k_+ is much smaller for benzene as compared to *n*-decane:

$$\frac{(k_+)_{\text{B}}}{(k_+)_{\text{D}}} = 2.3 \times 10^{-6}. \qquad [31]$$

Here and hereafter the subscripts "B" and "D" denote "benzene" and "decane," respectively. Below we will demonstrate that, from a physicochemical viewpoint, the higher activation-energy barrier for benzene can be attributed to the fact that the benzene molecules interact more favorably with the water molecules than the decane molecules. The latter is evidenced by the much higher solubility of benzene in water. Another indication in this aspect is the lower interfacial tension of the boundary benzene-water, $\sigma = 34.4$ mN/m, in comparison with that for decane-water, $\sigma = 51.2$ mN/m (at 20°C).

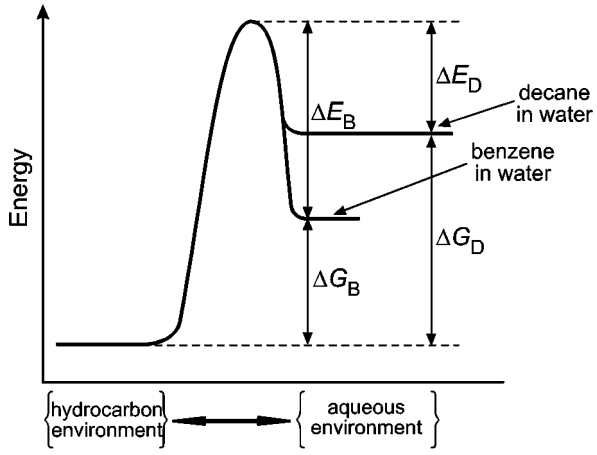

FIG. 8. Sketch of the kinetic barriers to transfer of a benzene ("B") or decane ("D") molecule from a hydrocarbon environment (bulk oil or micelle core) into an aqueous one, and vice versa.

From the viewpoint of formal kinetics, the lower solubilization rate constant of benzene could be interpreted as follows. The ratio of the two rate constants is

$$\frac{(k_+)_{\text{B}}}{(k_+)_{\text{D}}} = \exp[-(\Delta E_{\text{B}} - \Delta E_{\text{D}})/kT], \qquad [32]$$

where ΔE_{B} and ΔE_{D} denote the activation free energies for incorporation of a benzene or decane molecule into a surfactant micelle, see Fig. 8. On the other hand, the ratio of the equilibrium solubilities of these two hydrocarbons is

$$\frac{(c_{\text{eq}})_{\text{D}}}{(c_{\text{eq}})_{\text{B}}} = \exp[-(\Delta G_{\text{D}} - \Delta G_{\text{B}})/kT] = 4.9 \times 10^{-5}, \qquad [33]$$

where ΔG_{B} (or ΔG_{D}) denotes the free energy for transfer of a benzene (or a decane) molecule from hydrocarbon to aqueous environment. In Fig. 8 we illustrate that

$$\Delta E_{\text{B}} - \Delta E_{\text{D}} \approx \Delta G_{\text{D}} - \Delta G_{\text{B}} \qquad [34]$$

if we employ the simplifying assumption that the energy of an oil molecule in a "hydrocarbon environment" is approximately the same. Of course, the latter energy depends (i) on whether the molecule is benzene or decane and (ii) on the type of environment: aliphatic, aromatic, or micellar interior. This may explain the differences between the numbers in the right-hand sides of Eqs. [31] and [33].

The simplifying assumption that the energy of an oil molecule in a hydrocarbon environment is the same for all considered cases is equivalent to suppose that the barrier height stays the same for different oil types. Indeed, from a physical viewpoint, the energy in graphs like Fig. 8 is defined up to an arbitrary additive constant. Choosing this constant in such a way that the

point of the maximum coincides for benzene and decane, one will obtain, in general, different energy levels corresponding to benzene and decane in "aqueous environment" and "hydrocarbon environment," see the right- and left-hand-side levels in Fig. 8. The aforementioned assumption states that the left-hand-side energy levels coincide. Despite this obvious simplification, Eq. [34] indicates correctly the direction of the expected effect; that is,

$$\text{If } \frac{(c_{\rm eq})_{\rm D}}{(c_{\rm eq})_{\rm B}} \ll 1, \quad \text{then it follows } \frac{(k_+)_{\rm B}}{(k_+)_{\rm D}} \ll 1. \qquad [35]$$

In other words, the nonpolar oil (benzene), which exhibits a *greater* solubility in water, has a *smaller* rate constant of solubilization; i.e., it encounters a higher barrier to solubilization.

Next, we consider the effective (apparent) rate of solubilization, which is characterized by the rate of diminishing of the drop radius, $|dR/dt|$. For sufficiently large drops, $R \gg \kappa^{-1}$, and for relatively large mass-transfer coefficient, $\alpha/\kappa \gg 1$, Eq. [14] reduces to

$$|dR/dt| \approx \beta\kappa = \lambda v_{\rm oil} c_{\rm eq} (k_+ D_{\rm oil} c_{\rm tot})^{1/2}. \qquad [36]$$

Then from Eqs. [32]–[34] and [36] one obtains

$$\frac{|dR/dt|_{\rm D}}{|dR/dt|_{\rm B}} \propto \frac{\left(c_{\rm eq} k_+^{1/2}\right)_{\rm D}}{\left(c_{\rm eq} k_+^{1/2}\right)_{\rm B}} \approx \exp\left[-\frac{1}{2}(\Delta G_{\rm D} - \Delta G_{\rm B})/kT\right] = \left[\frac{(c_{\rm eq})_{\rm D}}{(c_{\rm eq})_{\rm B}}\right]^{1/2}. \qquad [37]$$

In other words, in a final reckoning it turns out that the oil, which exhibits a greater solubility in pure water, will be solubilized faster, irrespective of its smaller solubilization rate constant. Of course, in Eq. [37] "B" and "D" could be every two nonpolar liquid oils, which are solubilized by the discussed mechanism (not necessarily benzene and decane).

We recall that Eq. [37] is obtained by using two simplifying assumptions, viz. $\kappa R \gg 1$ and $\alpha/\kappa \gg 1$. The former assumption can be violated for benzene emulsion drops (Tables 3, 4), and leads to their faster diminishing due to a pronounced molecular oil solubility, see Fig. 5. The second assumption, $\alpha/\kappa \gg 1$, can be violated for drops of *n*-decane at sufficiently high micelle concentrations—in this case the rate of drop diminishing tends to level off, see Fig. 7.

5.3. Comparison between Experiments with Single Drops and Emulsions

Kinetics of solubilization can be investigated also in experiments with emulsions which are subjected to shaking or stirring (25, 11), or the oil droplets are of sub-micrometer size and are involved in Brownian motion (23, 26). One way to detect solubilization is to measure the turbidity of the emulsion, which allows one to characterize the rate of solubilization with the time needed for the turbidity to level off (25). More detailed kinetic information can be obtained if the time dependencies of the drop size and concentration are detected by dynamic and static light scattering (23, 26). Another method is to take samples from the shaken emulsion at selected times, and to subject the samples to phase separation using a centrifuge: the kinetics of solubilization is characterized by the decrease of the volume of the separated oily phase for subsequent samples (11). Below we specify the major physical differences between the solubilization experiments with emulsions (11, 23, 25, 26) and with single drops (Section 2 above).

First, in our experiments the solubilization of single drops happens under a pure diffusion regime, which enables one to determine the rate constant k_+ and the mass transfer coefficient α (for decane, see Eq. [28]), or only k_+ (for benzene, see Table 3). On the other hand, in solubilization experiments with emulsions the transfer of oil is dominated by the convections and, consequently, the speed of the process is limited by the rate of dissolution of oil molecules at the oil-water interface (26); hence, in such experiments one can determine only the mass-transfer coefficient (a counterpart of α, see below).

Second, in our experiments with single drops, the bulk aqueous phase (far from the drop) contains empty micelles all the time. In contrast, in the experiments with emulsions, the micelles are being gradually "filled" with oil until eventually reaching a complete saturation.

Third, to interpret quantitatively the solubilization experiments with emulsions one needs to know the area of the oil-water interface per unit volume of the emulsion, a_s. The latter varies with time due to the diminishing of the oil drops (23, 26). The dependence $a_s(t)$ can be influenced by effects like Ostwald ripening, drop flocculation, and coalescence, which lead to additional complicating of the physical picture. Such complications are missing in the experiments with single drops.

Despite the aforementioned differences, the solubilization experiments with single drops and emulsions are closely related and from their analysis one could extract mutually complementary information and verify the used model considerations. Investigation of the links between the two types of experiments demands a separate study involving parallel comparative measurements with single drops and emulsions, followed by a theoretical analysis which accounts for the complications noted above. Such investigation is out of the scope of the present article. Here, we consider only the connection between the mass-transfer coefficients determined by the two approaches, which enables one to verify the agreement between them, at least by order of magnitude. The following semiempirical equation was proposed to describe the solubilization process for O/W emulsions (11, 26),

$$\frac{\partial c_{\rm oil}}{\partial t} = k_{\rm f} a_s (c_{\rm sat} - c_{\rm oil}), \qquad [38]$$

where $c_{\rm oil}$ is the total concentration of oil in the aqueous phase, including that solubilized in the micelles; $c_{\rm sat}$ is the value of $c_{\rm oil}$

at saturation of the swollen micelles, k_f is an interfacial mass-transfer coefficient. Equation [38] must be compared with our Eq. [8], which implies

$$\frac{\partial c_{oil}}{\partial t} = a_s \left(-D_{oil} \frac{\partial c_{oil}}{\partial r} \right)_{r=R} = a_s D_{oil} \alpha (c_{eq} - c_{oil}). \quad [39]$$

Neglecting (in first approximation) some differences between the mechanisms of mass transfer behind Eqs. [38] and [39], we compare the latter equations to obtain

$$k_f \approx \frac{c_{eq}}{c_{sat}} D_{oil} \alpha. \quad [40]$$

For decane from Table 1 and Eq. [28] we take the values $D_{oil} = 7.8 \times 10^{-6}$ cm^2/s and $\alpha \approx 3 \times 10^5$ cm^{-1}; in addition, from Ref. (11) we take the values $c_{eq} = 0.052$ mg/dm^3 and $c_{sat} = 322$ mg/dm^3. With these parameter values from Eq. [40] we calculate $k_f = 1.4$ cm/h which is to be compared with the value $k_f = 3.6$ cm/h obtained in Ref. (11). This coincidence in the order of magnitude of k_f is encouraging, insofar as our value for α refers to SDS, whereas the values of k_f and c_{sat} from Ref. (11) correspond to the nonionic surfactant $C_{12}EO_{12}$ (polyoxyethylene-12-dodecyl ether). (Unfortunately, we could not find data for the rate of solubilization of decane in solutions of SDS.) In general, the values of k_f calculated from our α are close to the range of values measured by Prak *et al.* (11) for solubilization of decane in solutions of several nonionic surfactants.

Note also that all values of k_f and c_{sat} in Ref. (11) have been obtained for surfactant concentration 0.01 M. McClements and Dungan (26) established that k_f is independent of the surfactant concentration in the case of solubilization of *n*-hexadecane in micellar solutions of Tween 20.

5. CONCLUSIONS

(1) The obtained experimental data for the kinetics of solubilization of *n*-decane and benzene by SDS micelles agree very well with the proposed theoretical model, see Eqs. [17], [23], and [24] and Figs. 2–5.

(2) By processing the experimental data we determined the rate constant of solubilization, k_+, for a given oil and surfactant; see Eq. [29] and Tables 3 and 4. This parameter is important for the occurrence of solubilization under various types of experimental conditions, not necessarily in the absence of convection, as it is in our present study. In the case of *n*-decane it is possible to determine also the kinetic coefficient of transfer of oil molecules across the oil-water interface, α see Eqs. [8] and [28].

(3) The determined values of k_+ show that for both benzene and *n*-decane the elementary act of catching of a dissolved oil molecule by a surfactant micelle happens under a barrier (rather than diffusion) control; i.e., $k_+ \ll 4\pi D_{oil} r_m$. Hence, stirring is not expected to accelerate the micellar solubilization of oil molecules dissolved in water (no oil drops).

(4) However, stirring (convection) could accelerate the dissolution of oil from drops, if the thickness of the hydrodynamic boundary layer is comparable, or smaller, than the width of the solubilization "active zone," $\kappa^{-1} = [D_{oil}/(k_+ c_{tot})]^{1/2}$; see the values of κ in Tables 2–4.

(5) The analysis of the data for *n*-decane shows that all micelles turn out to be active; i.e., inactive full micelles are absent. As a result, in this case the rate of solubilization is independent of the diffusion coefficient of the micelles, but it is sensitive to the micelle concentration, c_{tot}, see Fig. 7.

(6) In contrast, the micellar solubilization of benzene occurs on the background of an intensive molecular dissolution of benzene in water. For lower micelle concentrations there are indications about the appearance of "full" micelles in the solution; see the discussion related to Tables 3 and 4.

(7) The rate constant k_+ turns out to be smaller for oils exhibiting higher solubility in pure water; in particular, k_+ is much less for benzene than for *n*-decane, see Eq. [31].

(8) The effective rate of solubilization of drops, $|dR/dt|$, is greater for the oil, which exhibits a higher equilibrium solubility in pure water, c_{eq}, irrespective of the smaller k_+ for this oil; for estimates one can use the relationship $|dR/dt| \propto (c_{eq})^{1/2}$, see Eq. [37]; possible reasons for a deviation from the latter relationship are also discussed in the text.

APPENDIX

In our experiments the oil drop is located below the glass surface (the inner wall of the capillary) due to the effect of buoyancy; see Fig. 1. The microscopic observations show that the drops ($R \leq 50$ μm) are almost perfectly spherical and that they do not stick to the glass wall; this indicates the presence of an aqueous film, which separates the drops from the glass. The diffusion transport in the vicinity of such a drop is affected by the presence of the glass wall. Our goal here is to estimate the deceleration of the diminishing of an oil drop located below a solid wall, in comparison with a similar drop situated in the bulk of solution. Since the radii of our drops are much smaller than the radius of the inner wall of the capillary, we will consider the simpler case of a drop located in the neighborhood of a planar wall, see Fig. 9. The xy plane of the coordinate system coincides with the solid surface, while the z axis is chosen to pass through the center of the spherical drop. We seek a solution, $c(x,y,z)$, of the equation,

$$\nabla^2 c = \kappa^2 c, \quad [A1]$$

satisfying the boundary condition

$$(\partial c/\partial z)_{z=0} = 0. \quad [A2]$$

Equation [A2] means that the diffusion flux across the plane $z = 0$ (the solid surface) is zero. For the sake of brevity here and hereafter we skip the subscript "oil" of quantities as c, D,

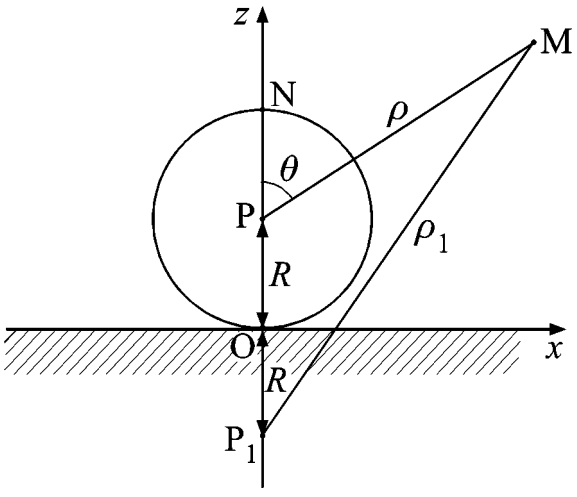

FIG. 9. Sketch of a spherical oil drop in contact with a solid surface; ρ and ρ_1 are, the distances from a point M to the center of the sphere P and its mirror image P_1, respectively.

etc. One can check that the solution of the boundary problem [A1]–[A2] is

$$c = A\left[\frac{\exp(-\kappa\rho)}{\rho} + \frac{\exp(-\kappa\rho_1)}{\rho_1}\right], \qquad [A3]$$

where A is a constant of integration, and

$$\rho = [x^2 + y^2 + (z-R)^2]^{1/2}, \quad \rho_1 = [x^2 + y^2 + (z+R)^2]^{1/2}. \qquad [A4]$$

In fact, ρ and ρ_1 represent the distances from a point M, where the concentration c is evaluated, to the center of the sphere, P, and to its mirror image P_1; see Fig. 9. Next, we introduce polar coordinates (r,θ,φ) with origin in the center of the spherical drop (point P in Fig. 9). In terms of these coordinates Eq. [A4] acquires the form

$$\rho = r, \quad \rho_1 = (r^2 + 4Rr\cos\theta + 4R^2)^{1/2}. \qquad [A5]$$

To determine the constant A, we assume that the flux at the upper point of the drop, point N in Fig. 9, is the same as for a drop of the same radius in the bulk:

$$-D\left.\frac{\partial c}{\partial r}\right|_{r=R;\theta=0} = Q. \qquad [A6]$$

Substituting Eq. [A3] into [A6] we determine

$$A = \frac{QR^2/D}{1 + \kappa R + \frac{1}{9}(1+3\kappa R)\exp(-2\kappa R)}. \qquad [A7]$$

For an arbitrary θ, the flux of oil molecules per unit area of the surface of the drop in Fig. 9 can be expressed in the form

$$\tilde{Q}(\theta) = -D\left.\frac{\partial c}{\partial r}\right|_{r=R} = A_1\left[\left(\frac{1}{R^2} + \frac{\kappa}{R}\right) - \frac{d}{d\rho_1}\left(\frac{1}{\rho_1}e^{\kappa(R-\rho_1)}\right)\frac{\partial\rho_1}{\partial r}\right]_{r=R}, \qquad [A8]$$

where

$$A_1 = AD\exp(-\kappa R). \qquad [A9]$$

The average value of the flux of oil molecules across the oil-water interface is

$$\bar{Q} = \frac{1}{4\pi R^2}\int_0^{2\pi} d\varphi \int_0^{\pi} d\theta\, R^2 \sin\theta\, \tilde{Q}(\theta). \qquad [A10]$$

Further, we substitute Eq. [A8] into [A10]; the integration can be carried out analytically with the help of the following auxiliary relationship:

$$\left.\frac{\partial\rho_1}{\partial r}\right|_{r=R} = \left(\frac{1}{2R} + \frac{\cos\theta}{R}\right)\left.\frac{\partial\rho_1}{\partial(\cos\theta)}\right|_{r=R}. \qquad [A11]$$

The result of integration reads

$$\bar{Q} = \lambda Q \qquad [A12]$$

$$\lambda = \frac{3 + 4\kappa R - \exp(-2\kappa R) + [1 - \exp(-2\kappa R)]/(\kappa R)}{4[1 + \kappa R + \frac{1}{9}(1+3\kappa R)\exp(-2\kappa R)]}. \qquad [A13]$$

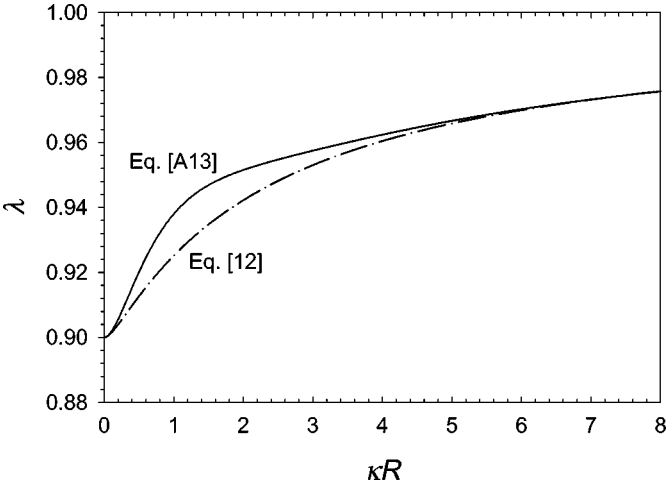

FIG. 10. Comparison of the exact and approximate curves $\lambda(\kappa R)$ calculated, respectively, by means of Eqs. [A13] and [13].

The function $\lambda(\kappa R)$ has the following asymptotic behavior

$$\lambda = 0.9 + 0.21(\kappa R)^2 + O[(\kappa R)^3], \quad (\kappa R \ll 1) \qquad [A14]$$

$$\lambda = 1 - 0.25(\kappa R)^{-1} + O[(\kappa R)^{-2}], \quad (\kappa R \gg 1). \qquad [A15]$$

It is convenient to approximate $\lambda(\kappa R)$ with a simpler expression, which has the same asymptotic behavior; such expression is given by Eq. [13]. In Fig. 10 we compare the curves $\lambda(\kappa R)$ calculated by means of Eqs. [13] and [A13]. One sees that Eq. [13] provides a good approximation for the function $\lambda(\kappa R)$ defined by Eq. [A13].

ACKNOWLEDGMENTS

This work was supported in part by Colgate-Palmolive Co. and in part by Inco-Copernicus Project No. IC15 CT98 0911 of the European Commission. The authors are indebted to Mr. George Marinov for his contribution to the development of the experimental technique, to Prof. Ivan B. Ivanov for the critical reading of the manuscript, and to Prof. Krassimir Danov for his help in the data processing.

REFERENCES

1. Plucinski, P., and Nitsch, W., *J. Phys. Chem.* **97,** 8983 (1993).
2. Chan, A. F., Evans, D. F., and Cussler, E. L., *AIChE J.* **22,** 1006 (1976).
3. Carroll, B. J., *J. Colloid Interface Sci.* **79,** 126 (1981).
4. Ward, A. J., *in* "Solubilization in Surfactant Aggregates" (S. D. Christian and J. F. Scamehorn, Eds.), p. 237. Dekker, New York, 1995.
5. Miller, C. A., *in* "Handbook of Surface and Colloid Chemistry" (K.S. Birdi, Ed.), p. 157. CRC Press, Boca Raton, FL, 1997.
6. Chen, B.-H., Miller, C. A., and Garrett, P. R., *Colloids Surf. A* **128,** 129 (1997).
7. Williams, C. L., Bhakta, A. R., and Neogi, P., *J. Phys. Chem. B* **103,** 3242 (1999).
8. Kabalnov, A., *J. Dispersion Sci. Technol.* **22,** 1 (2001).
9. Kabalnov, A., and Weers, J., *Langmuir* **12,** 3442 (1996).
10. Mayer, A. S., Zhong, L., and Pope, G. A., *Environ. Sci. Technol.* **33,** 2965 (1999).
11. Prak, D. J. L., Abriola, L. M., Weber, W. J., Jr., Bocskay, K. A., and Pennell, K. D., *Environ. Sci. Technol.* **34,** 476 (2000).
12. Todorov, P. D., Marinov, G. S., Kralchevsky, P. A., Denkov, N. D., Broze, G., and Mehreteab, A., submitted for publication.
13. Alargova, R. G., Danov, K. D., Kralchevsky, P. A., Broze, G., and Mehreteab, A., *Langmuir* **14,** 4036 (1998).
14. Birdi, K. S., Chapter 3 *in* "Handbook of Surface and Colloid Chemistry" (K. S. Birdi, Ed.), p. 97. CRC Press, Boca Raton, 1997.
15. Weiss, J., Coupland, J. N., and McClements, D. J., *J. Phys. Chem.* **100,** 1066 (1996).
16. Weiss, J., Coupland, J. N., Brathwaite, D., and McClements, D. J., *Colloids Surf. A* **121,** 53 (1997).
17. Weiss, J., and McClements, D. J., *Langmuir* **16,** 5879 (2000).
18. Lim, J.-C., and Miller, C. A., *Langmuir* **7,** 2021 (1991).
19. Chen, B.-H., Miller, and C. A., Garrett, P. R., *Langmuir* **14,** 31 (1998).
20. Mysels, K. J., *Langmuir* **8,** 3191 (1992).
21. Landau, L. D., and Lifshitz, E. M., "Fluid Mechanics." Pergamon, Oxford, 1984.
22. Reiss-Husson, F., and Luzzati, V., *J. Phys. Chem.* **63,** 1969 (1959).
23. Coupland, J. N., Brathwaite, D., Fairley, P., and McClements, D. J., *J. Colloid Interface Sci.* **190,** 71 (1997).
24. Bourrel, M., and Schechter, R. S., "Microemulsions and Related Systems," Dekker, New York, 1988.
25. Chiu, Y. C., and Chang, C. Y., *J. Surf. Sci. Technol.* **6,** 349 (1990).
26. McClements, D. J., and Dungan, S. R., *Colloids Surf. A* **104,** 127 (1995).